LOBE AND CLEFT FORMATION AT THE HEAD OF A GRAVITY CURRENT

J. N. McElwaine & M. D. Patterson
Department of Applied Mathematics and Theoretical Physics, Centre for Mathematical Sciences, University of Cambridge, Wilberforce Road, Cambridge CB3 0WA, England.

Summary Experiments have been carried out to examine the formation, and subsequent evolution, of lobes and clefts at the head of a gravity current. This has been achieved by calculating the curvature of the level-set of first-arrival times of the front. The results show that there is a weak dynamical linear instability when the radius curvature of the front is similar to the height. The formation and evolution of the clefts is then a nonlinear kinematic phenomenon, caused by the front propagating with a roughly constant normal velocity. Three different mechanisms for the initial instability are discussed and the subsequent evolution of the front is explained in detail.

INTRODUCTION

Gravity currents are a commonly occurring environmental flow and arise in a variety of situations, examples include the buoyancy-driven exchange through an open doorway, the spill of a dense gas, or a pyroclastic flow from a volcano. The density differences driving the flow may have their origins in temperature, composition, or the presence of suspended particles that sediment out of the advancing flow.

The general dynamics of a two-dimensional (2D) gravity current are now thought to be well understood. Laboratory experiments (5) have provided detailed observations of such flows. It was found that the flow arising after the release can be divided into a number of different phases. In the initial phase sometimes referred to as the 'slumping phase' the current develops and forms a head. Somewhat later, the gravity current reaches a second, self-similar phase, where there is a buoyancy-inertia balance. After sufficient time the flow will enter a final phase, in which it is governed by a buoyancy-viscous balance which is well described by shallow water theory.

While the general dynamics of 2D gravity currents are accurately described by relatively simple analysis, no information about the formation of the complicated three-dimensional (3D) lobe and cleft structures at the gravity currents head is provided by these models. Simpson (4) has carried out an experimental study on lobe and cleft formation where he photographed the gravity currents head from below and was thus able to track the clefts as they grew and merged. He suggested that the formation of lobes and clefts is due to the overrunning of less dense fluid by the dense gravity current, which in turn forces itself upward through the gravity current causing a cleft to form. Other work by Härtel (1) used 3D direct numerical simulations (DNS) of a gravity current at relatively low Reynolds number. The simulation exhibited all features typically observed in experimental flows near the gravity current head, including the lobe and cleft structure at the leading edge. The original work was furthered (2) with an examination of the lobe and cleft instability of a gravity current using linear-stability analysis. They concluded that there was a local linear instability at the leading edge of the front caused by the unstable stratification in the flow region between the nose and the stagnation point.

RESULTS

A series of laboratory experiments have been carried out in a glass tank 2.5 m $\times$ 0.7 m $\times$ 0.8 m. In the experiments the tank was filled with fresh water of density $\rho_A = 1000$ kg/m^3 to a depth H. A fixed volume of a denser saline solution of density ρ_L of the same depth, was kept behind a vertical barrier at a distance $L = 0.3$ m from the end of the tank. For visualisation purposes the dense fluid was dyed with food colouring. By lifting the barrier the denser fluid is released into tank. Illumination from behind and above using a diffuse light bank resulted in a sharply defined interface between the gravity current and the ambient fluid.

Video sequences of the experiments were analysed using the method developed in McElwaine (3). The arrival time $T(x, y)$ of the flow is detected for each pixel on the screen. This matrix $T(x, y)$ of first arrival times is a level set, since the contours $T(x, y) = t$ correspond to the front of the flow at a particular time. One such contour is shown in figure 1(a), where the accuracy of the method and the characteristic lobe and cleft structure can be clearly seen. Properties of the flow such as average front position and velocity can then be calculated directly from the contours and the movement of clefts and lobes can also be visualised. However, local features can most easily be tracked working directly with the level set. In general one should account for camera distortion before processing, but a large focal length lens was used and the camera axis was orthogonal to the plane of motion, so the relation between pixel coordinates and world coordinates is accurately represented by a simple scaling. Resampling errors can thus be avoided by working directly with pixel coordinates. The lobes corresponds to large regions of small positive curvature and the clefts to lines of large negative curvature. The curvature is defined as $\kappa = \nabla \cdot \frac{\nabla T}{|\nabla T|}$. Figure 1(b) shows the curvature of the level set from the experiment shown in Figure 1(a).

The structure and motion of the clefts is clearly seen in figure 1(c). The clefts appear and then slowly propagate along the front until they merge with other clefts. The most important point about clefts is that they are a *generic, kinematic* feature of system with evolving fronts that have nothing to do with dynamics. That is any system where the front propagates with approximately constant velocity normal to the front will develop clefts. These clefts correspond to a shock where two

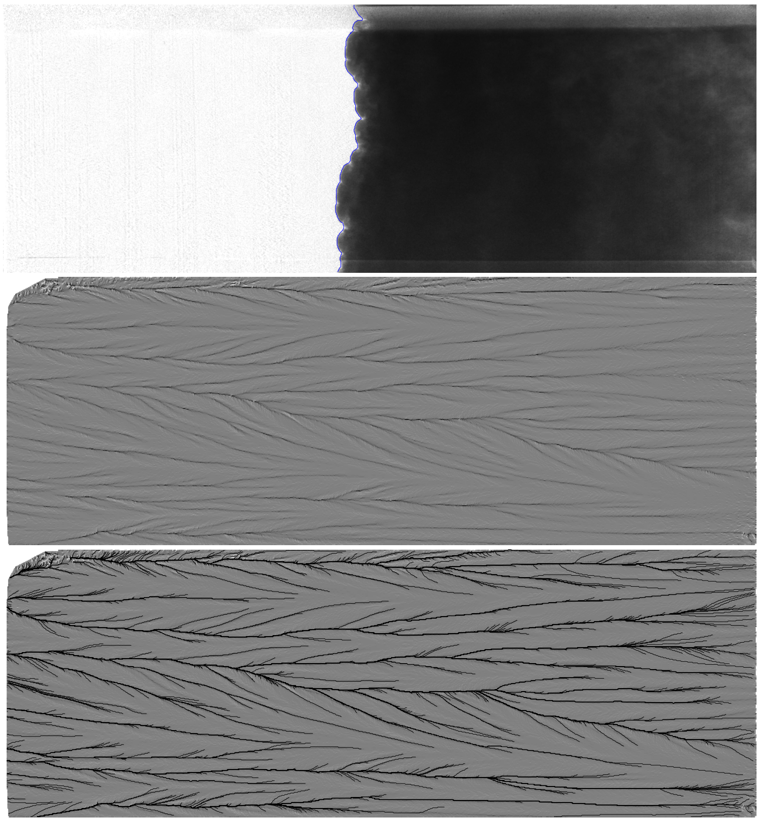

Figure 1. a) Contour mapping. The motion of the gravity current in all figures is right to left. b) Curvature of first arrival time field. Black corresponds to curvatures less than -2 (inverse pixels), white to great than +2, and the intensity is linear in between. c) Position of clefts superimposed on curvature picture

characteristics collide. As the front continues to propagate clefts can merge but never disappear. As the lobes between the clefts increases in size and decrease in curvature they become dynamically unstable and indent smoothly. After propagating a distance of the radius of curvature of the indentation a shock forms and a cleft appears. Thus the overall process is one of clefts continually forming and then merging but never disappearing as can be seen in figure 1(c).

Simpson's previous work states that lobe and cleft instability does not arise in the slip-boundary condition case and hence the instability is due to the overrunning of ambient fluid. This is not necessarily the case however. Compared to environmental flows experiments and simulations are performed at very low Reynolds numbers, where the flows are only barely turbulent. At higher Reynolds numbers the overrunning layer will increase in size relative to trapped ambient layer (scaling as $1/\sqrt{\mathrm{Re}}$) making the trapped layer less important. Since lobes and clefts are still observed for these flows there must at the very least be one other source of instability. An alternative explanation of the results of (4) is that with a slip boundary there is much less turbulence in the flow, and one would have to go to much higher Reynolds number to observe the instability. The scaling of this mechanism also seems wrong. As the flow increases in size and the Reynolds number increases the overrun layer shrink in thickness and one might expect the scale of the instability to scale with this.

Although only one of these seems to have received much attention in the literature. At least three possible mechanisms for generating the initial negative curvature leading to cleft formation appear to be possible, they will be described along with experimental evidence.

References

[1] HÄRTEL, C., MEIBURG, E. & NECKER, F. 2000 alysis and direct numerical simulation of the flow at a gravity-current head. part 1. flow topology and front speed for slip and non-slip boundaries. *J. Fluid Mech.* **418**, 189.

[2] HÄRTEL, C., MEIBURG, E. & NECKER, F. 2000 Analysis and direct numerical simulation of the flow at a gravity-current head. part 2. the lobe and cleft instability. *J. Fluid Mech.* **418**, 213.

[3] MCELWAINE, J. N. 2003 Image analysis for avalanches. To appear. Proceedings of International Seminar on Snow Avalanches Experimental Sites, Grenoble 2001.

[4] SIMPSON, J. E. 1972 Effects of the lower boundary on the head of a gravity current. *J. Fluid Mech.* **53**, 759-768.

[5] SIMPSON, J. E. 1997 *Gravity currents in the environment and the laboratory*. Cambridge University Press.